Alternate Pathways for Acetic Acid and Acetate ion Release from Acetylcholinesterase: a Molecular Dynamics Study

Istvan J. Enyedy,[†] Ildiko M. Kovach,*[,†] and Bernard R. Brooks[‡]

Contribution from the Department of Chemistry, The Catholic University of America, Washington, DC 20064, and Laboratory of Biophysical Chemistry, National Heart, Lung, and Blood Institute, The National Institutes of Health, Bethesda, Maryland 20892-5626

Received September 5, 1997

Abstract: Two competing passageways for the exit of acetic acid and acetate ion in *Torpedo californica (Tc)* acetylcholinesterase (ACHE) were studied by examining free energies of passage through two potential trajectories using the umbrella sampling technique as implemented in CHARMM. The coordinates for migration were defined as the distance from Ser200 Oγ, one through the 20-Å long active-site gorge ending with Trp279 and a 14-Å long route ending at Arg244. The free energies were calculated in successive windows 0.5 Å wide for 40−90 ps. The potential of mean force (PMF) was calculated along the coordinate for migration. The PMF for the migration of acetic acid decreases by ∼8 kcal/mol after 8-Å travel through the main gorge. The PMF profile for acetate ion migration falls to a 6 kcal/mol lower value than for acetic acid migration in the main gorge. The free energy barrier for the migration of acetate ion is 1.5 kcal/mol due to a constriction formed by Tyr121, Phe290, Phe330, and Phe331 in the main gorge. The interaction between acetic acid/acetate ion and the OH group of Tyr121 appears to guide product release through the main gorge. Acetate ion remains hydrogen-bonded to Tyr121 until it approaches Trp279 when it is expelled into bulk water. Acetic acid encounters a 6 kcal/mol barrier through the alternate pathway, while the PMF for acetate ion drops ∼27 kcal/mol when it approaches Arg244. This is the lowest energy path. Full molecular dynamics simulations, free of restraint for 170 ps, result in the migration of acetate ion through the short channel but not through the main gorge. The results indicate that if the nascent acetic acid should ionize within 3.5 Å from Ser200 Oγ, it would be more likely to exit via the alternate channel than through the main gorge.

Acetylcholinesterase (ACHE) fulfills its role to rapidly hydrolyze the neurotransmitter acetylcholine by catalyzing the reaction at low ionic strength with a bimolecular rate constant, k_{cat}/K_m, near the rate constant for diffusion.[1,2] The reaction sequence most consistent with experimental data to date involves double nucleophilic displacements with the intermediacy of a covalent acetyl enzyme and two proton-transfer steps in each phase. Scheme 1 gives an account of the events, without details of elementary steps inclusive in *K*, in the initial phase of the reaction.[1]

Under complete substrate saturation, $k_{cat} = k_2k_3/(k_2 + k_3)$ and $k_3 = 0.68k_2$ for electric eel AChE at pH 7.0 and 23 °C, indicating that deacylation is 68% and acylation is 32% rate determining.[1,3,4] Product inhibition of cholinesterases either by choline or by acetate ion has not been reported. An important aspect of the high efficiency of AChE function is the elucidation of the pathway(s) for product release from the active site. The X-ray structure of a monomer of the dimeric *Torpedo californica (Tc)* AChE[5] revealed that the active site of the enzyme is situated at the bottom of a 20-Å-deep hydrophobic gorge.[2,5] This then raises the question how substrate and products travel in and out efficiently under all conditions. Two other facts point to the existence of an alternate exit channel(s): The symmetry-related copy of the monomer blocks the entrance to the active-site gorge in the crystal structure yet ligands could diffuse into the active site.[6,7] A more recent X-ray structure of mouse (Mo) AChE complexed with fasciculin,[8] a snake toxin, shows a

Scheme 1

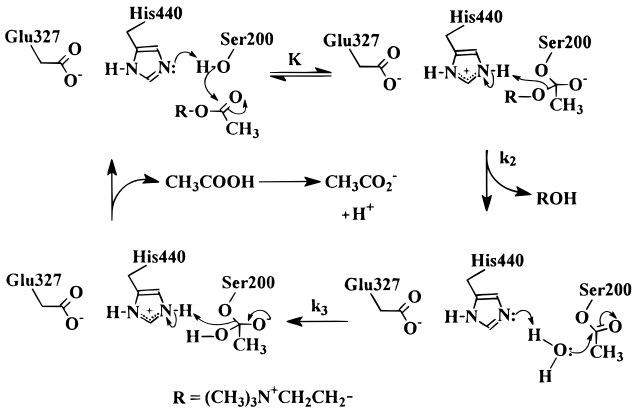

[†] The Catholic University of America.
[‡] The National Institutes of Health.

(1) Quinn, D. M. *Chem. Rev.* **1987**, *87*, 955−975.
(2) Harel, M.; Quinn, D. M.; Nair, H. K.; Silman, I.; Sussman, J. L. *J. Am. Chem. Soc.* **1996**, *118*, 2340−2346.
(3) Froede, H. C.; Wilson, I. B. *J. Biol. Chem.* **1984**, *259*, 11010−11013.
(4) Kovach, I. M.; Larson, M.; Schowen, R. L. *J. Am. Chem. Soc.* **1986**, *108*, 3054−3056.
(5) Sussman, J. L.; Harel, M.; Frolow, F.; Oefner, C.; Goldman, A.; Toker, L.; Silman, I. *Science* **1991**, *253*, 872−879.
(6) Axelsen, P. H.; Harel, M.; Silman, I.; Sussman, J. L. *Protein Sci.* **1994**, *3*, 188−197.
(7) Harel, M.; Schalk, I.; Ehret-Sabatier, L.; Bouet, F.; Goeldner, M.; Hirth, C.; Axelsen, P.; Silman, I.; Sussman, J. L. *Proc. Natl. Acad. Sci. U.S.A.* **1993**, *90*, 9031−9035.
(8) Bourne, Y.; Taylor, P.; Marchot, P. *Cell* **1995**, *83*, 503−512.

S0002-7863(97)03131-4 CCC: $15.00 © 1998 American Chemical Society
Published on Web 07/30/1998

completely blocked active-site gorge by the inhibitor. Yet the active-site Ser of the complex reacts with inhibitors[9] and substrates[10,11] at 0.1−5% activity of the native enzyme. The fasciculin-inhibited Mo AChE has an active site somewhat distorted and displaced toward the Ω loop which seems to have a key role in enzyme function.

Fascination with substrate entry and product release, a key issue of enzymic reaction dynamics, led to investigations using computational techniques[6,7,12−20] immediately after publication of the X-ray coordinates of the monomer of *Tc* AChE.[5] A 120-ps molecular dynamics (MD) simulation of the solvated native *Tc* AChE did not detect permeability of the protein.[14] However, a surface analysis revealed after the first 20 ps, a brief 0.3-ps opening in the thin wall at Trp84 while the indole side chain of Trp84 rotated. Although the aperture was large enough for the passage of a water molecule only, the possibility for a more significant opening while performing catalysis at a longer time scale has not been precluded. Effector-induced conformational changes in the enzyme can widen crevices and holes into passageways.

An exploratory grid search algorithm for mapping the channels which connect the active site to the protein exterior was developed in this laboratory and published.[21] It located *one* alternate route, to the main gorge, for the release of acetate ion in the direction of a surface depression. The surface depression is lined with positively charged residues. Although the channel is narrow for the passage of product fragments, it appeared that a conformational change could cause the breakage of a salt bridge and the formation of two other salt bridges that would allow widening of the opening. A subsequent adiabatic search for feasible pathways for product clearance showed that the alternate pathway for acetic acid release may not even require a major conformational change. Instead, the widening of the aperture could easily be triggered by bond breaking in the quasitetrahedral transition state for the hydrolysis of acetyl enzyme in the last step of the reaction sequence. It appeared that significant gating motions of side chains may be coupled with slight conformational changes in the backbone. These small local adjustments in side chains and main chains generally do not alter the overall features of the protein as shown by Karplus.[17,22−25] An adiabatic description could provide approximate potential energy barrier heights[26] to the passage of products. If the barrier height is such that minor skeletal fluctuations may eliminate it, then the protein can be relaxed within the adiabatic limit in the presence of the perturbing fragment. The fragment needs to be held by a restraining shallow harmonic potential adjusted according to the curvature of the trajectory during the dynamic simulation. The calculation can then be extended under diabetic conditions. Umbrella sampling along the coordinate for migration, within program CHARMM,[27] was chosen to accomplish the task and to calculate free energies for the exit of products.[23,25,28−36]

The electrostatic properties of acetic acid should change substantially on ionization as shown in Scheme 1. Consequently, an evaluation of the release of acetate ion from AChE would have to begin with the question at which point ionization of acetic acid, as shown in Scheme 1, may occur. In all likelihood, ionization occurs on first encounter with a lone pair of electrons on a protein acceptor or solvate water, however, the persistence of acetic acid in a hydrophobic environment cannot be ruled out. In this investigation, the exit of acetic acid and acetate ion through the entrance gorge were compared with their exit via another plausible channel from the protein. The free energy barriers were characterized, and the amino acid residues that may facilitate or thwart product release were identified by calculating interaction energies between them and acetic acid or acetate ion.

Methods

Most of the calculations were carried out on Cray C90, J90, or T3E computers at the Pittsburgh Supercomputing Center. Preliminary calculations were done on an SGI Indigo 2 workstation. Molecular dynamics program CHARMM[27] was used with the all-atom parameter set[37,38] and a constant dielectric ($\epsilon = 1$). The modified TIP3P solvation model was used.[39,40] Long-range electrostatic forces were treated with

(9) Marchot, P.; Khelif, A.; Ji, Y. H.; Mansuelle, P.; Bougis, P. E. *J. Biol. Chem.* **1993**, *268*, 12458−12467.
(10) Radic, Z.; Quinn, D. M.; Vellom, D. C.; Camp, S.; Taylor, P. *J. Biol. Chem.* **1995**, *270*, 20391−20399.
(11) Radic, Z.; Duran, R.; Vellom, D. C.; Li, Y.; Chambers, J. L.; Taylor, P. *J. Biol. Chem.* **1993**, *269*, 11233−11239.
(12) Tan, R. C.; Truong, T. N.; McCammon, J. A.; Sussman, J. L. *Biochemistry* **1993**, *32*, 401−403.
(13) Harel, M.; Sussman, J. L.; Krejci, E.; Bon, S.; Chanal, P.; Massoulie, J.; Silman, I. *Proc. Natl. Acad. Sci. U.S.A.* **1992**, *89*, 10827−10831.
(14) Gilson, M. K.; Straatsma, T. P.; McCammon, J. A.; Ripoll, D. R.; Faerman, C. H.; Axelsen, P. H.; Silman, I.; Sussman, J. L. *Science* **1994**, *263*, 1276−1278.
(15) Ripoll, D. L.; Faerman, C. H.; Axelsen, P. H.; Silman, I.; Sussman, J. L. *Proc. Natl. Acad. Sci. U.S.A.* **1993**, *90*, 5128−5131.
(16) Antosiewicz, J.; Gilson, M. K.; McCammon, J. A. *Isr. J. Chem.* **1994**, *34*, 151−158.
(17) Antosiewicz, J.; Gilson, M. K.; Lee, I. H.; McCammon, J. A. *Biophys. J.* **1995**, *68*, 62−68.
(18) Antosiewicz, J.; McCammon, J. A.; Wlodek, S. T.; Gilson, M. K. *Biochemistry* **1995**, *34*, 4211−4219.
(19) Wlodek, S. T.; Antosiewicz, J.; Briggs, J. M. *J. Am. Chem. Soc.* **1997**, *119*, 8159−8165.
(20) Wlodek, S. T.; Clark, T. W.; Scott, L. R.; McCammon, J. A. *J. Am. Chem. Soc.* **1997**, *119*, 9513−9522.
(21) Kovach, I. M.; Qian, N. F.; Bencsura, A. *FEBS Lett.* **1994**, *349*, 60−64.
(22) Karplus, M.; McCammon, J. A. *CRC Crit. Rev. Biochem.* **1981**, 293−349.
(23) McCammon, J. A.; Karplus, M. *Proc. Natl. Acad. Sci. U.S.A.* **1979**, *76*, 3585−3589.
(24) Brooks, C. L., III; Brunger, A.; Karplus, M. *Biopolymers* **1985**, *24*, 843−865.
(25) Case, D. A.; Karplus, M. *J. Mol. Biol* **1979**, *132*, 343−368.
(26) Warshell, A.; Levitt, M. *J. Mol. Biol.* **1976**, *103*, 227−249.
(27) Brooks, B. R.; Bruccoleri, R. E.; Olafson, B. D.; States, D. J.; Swaminathan, S.; Karplus, M. *J. Comput. Chem.* **1983**, *4*, 187−217.
(28) Northrup, S. H.; Pear, M. R.; Lee, C.-Y.; McCammon, J. A.; Karplus, M. *Proc. Natl. Acad. Sci. U.S.A.* **1982**, *79*, 4035−4039.
(29) Case, D. A.; McCammon, J. A. *Ann. N. Y. Acad. Sci.* **1986**, *482*, 222−233.
(30) Kottalam, J.; Case, D. A. *J. Am. Chem. Soc.* **1988**, 110, 7690−7697.
(31) Brooks, C. L., IlI; Karplus, M.; Pettitt, B. M. In *Proteins. A Theoretical Perspective of Dynamics, Structure, and Thermodynamics;* Wiley & Sons: New York, 1988; pp 46−49.
(32) Beveridge, D. L.; DiCapua, F. M. *Annul Rev. Biophys. Chem.* **1989**, *18*, 431−492.
(33) Young, W. S.; Brooks, C. L., III. *J. Mol. Biol.* **1996**, *230*, 560−573.
(34) Brooks, C. L., III; Case, D. A. *Chem. Rev.* **1993**, 2487−2502.
(35) Tobias, D. J.; Brooks, C. L., III. *Biochemistry* **1991**, *30*, 6059−6070.
(36) Torrie, G. M.; Valleau, J. P. *J. Comp. Phys.* **1977**, *23*, 187-199.
(37) MacKerell, A. D., Jr.; Bashford, D.; Bellott, M.; Dunbrack, R. L. J.; Field, M. J.; Fischer, S.; Gao, J.; Guo, H.; Ha, S.; Joseph, D.; Kuchnir, L.; Kuczera, K.; Lau, F. T. K.; Mattos, C.; Michnick, S.; Nguyen, D. T.; Ngo, T.; Prodhom, B.; Roux, B.; Schlenkrich, M.; Smith, J.; Stote, R.; Straub, J.; Wiorkiewicz-Kuczera, J.; Karplus, M. *FASEB J.* **1992**, *6*, A143.
(38) MacKerell, A. D., Jr.; Bashford, D.; Bellott, M.; Dunbrack, R. L., Jr.; Evanseck, J.; Field, M. J.; Fischer, S.; Gao, J.; Guo, H.; Ha, S.; Joseph, D.; Kuchnir, L.; Kuczera, K.; Lau, F. T. K.; Mattos, C.; Michnick, S.; Ngo, T.; Nguyen, D. T.; Prodhom, B.; Reiher, I. W. E.; Roux, B.; Schlenkrich, M.; Smith, J.; Stote, R.; Straub, J.; Watanabe, M.; Wiorkiewicz-Kuczera, J.; Yin, D.; Karplus, M. Unpublished data.
(39) Jorgensen, W. L.; Chandrasekhar, J.; Madura, J. D.; Impey, R. W.; Klein, M. L. *J. Chem. Phys.* **1983**, *79*, 926−935.

the force switch method[41] in a switching range of 8−12 Å. van der Waals forces were calculated with the shift[41] method and a cutoff of 12 Å. The nonbond list was kept to 14 Å and updated heuristically. A step size of 1 fs was used in all calculations.

Structure Preparation. The starting coordinates were taken from the entry lACE[5] in the Brookhaven Data Bank.[42] The missing side chains and residues 485−489 were built using the standard values from the parameter file for the internal coordinates. Residues 1−3 and 535−537 missing from the structure were not reconstructed. Hydrogen atoms were added using the HBUILD[43] routine of CHARMM. Acidic and basic residues were given unit electrostatic charges. All Tyr and Cys residues were neutral. The site of protonation of the His residues were based on the availability of hydrogen (H)-bond donors or acceptors and were identical to those published earlier.[44−46] His440 was protonated on Nδ.

The structure was then solvated by placing it in an equilibrated box of water molecules.[47] All water molecules which were not in the crystal structure and those with oxygens at least 2.5 Å from the nearest protein atom or farther than 6.0 Å from an atom were deleted.[48] This minimal solvation was shown to sufficiently stabilize the protein structure in a 100-ps MD simulation.[49] A total of 2942 water molecules (8826 atoms) were equilibrated at 300 K for 10 ps, while keeping the 8339 protein atoms and the 69 crystallographic water molecules fixed. This allowed for an optimal distribution of water molecules on the protein surface. The whole structure was further energy-minimized. This was followed by a 120-ps MD simulation.

Umbrella Sampling. To reduce the required computation time and to eliminate possible slowly relaxing energy fluctuations outside the region of interest, simulations were done with the stochastic boundary method.[24,50,51] The system was divided into reaction and buffer regions. Residues outside these regions were deleted. A region of 23-Å radius around the middle point between residues Ser200 and Trp279 was the reaction zone. This included the entire alternate channel with the requisite solvent shell in the groove. A 2.0-Å buffer region surrounding the reaction region underwent Langevin dynamics to allow energy to flow in to and out of the reaction region.[22,27,52] Frictional coefficients of water oxygen and heavy atoms in the protein were set to 62 and 200 ps^{-1}, respectively.[53] Protein atoms in the buffer zone but originating outside the 2-Å range were constrained to their initial positions. Acetic acid and acetate ion were generated using standard values from the parameter file.

A preliminary adiabatic molecular mechanics search confirmed that an exit channel other than the main gorge was feasible. Thus, two channels were studied: One through the entrance gorge and another channel in the direction of Arg244. The distance between Ser200 Oγ and the carbonyl carbon of the product was used as coordinate for migration, δ, for product release through the main gorge. The distance between Arg244 Nη2 and the carbonyl carbon was used as the coordinate for product release through the alternate exit. This coordinate was transformed to δ values consistent with the definition given for the main gorge. Since the active-site residues are among the most still residues in the enzyme, Ser200 Oγ is a good choice of reference for migration. Although Arg244 Nη2 may move during the simulation, it too was an adequate reference point as indicated by reproducible results of repeated simulations and a barrierless minimum energy pathway (vide infra).

The starting structure was derived from the quasitetrahedral transient preceding C−O bondbreaking and the formation of acetic acid. The structure of nascent acetic acid was positioned at a bond order of 0.009, 2.8 Å, for the C−O bond between Ser Oγ and the carbonyl carbon. The orientation of acetic acid was kept the same as in its quasitetrahedral adduct precursor. This structure was minimized first while applying a restraining force on all protein atoms. A second minimization followed with an additional restraint for keeping the distance between Ser200 Oγ and carbonyl carbon of acetic acid constant.

The free energy profiles for acetic acid/acetate ion diffusion through the two pathways were calculated using the umbrella sampling technique.[23,25,28−36] A quadratic biasing potential, $U(\delta) = K(\delta - \delta_o)^2$, was used to hold the acetate ion within the specified region. The force constant was set to $K = 5$ kcal/mol Å^2.

The energy-minimized starting structure was equilibrated at 300 K and the biasing potential minimum was placed at 3 Å for 90 ps. This allowed for full conformational and solvent equilibration around acetic acid at a total root-mean-square deviation (RMSD) < 0.5 Å in the first window. For optimal sampling of different positions of the product, the minimum of the biasing potential was shifted in the desired direction, forward or backward, along δ by 0.5 Å for each window. Umbrella sampling starting structures for each window were prepared by the translation of the acetic acid/acetate ion by 0.5 Å in the direction of the desired pathway. After two windows, at $\delta = 4$ Å, two parallel second steps were taken: (A) in the direction of the main gorge and (B) in the direction toward Arg244. Figure 1 illustrates the starting orientation of acetic acid and the subsequent two steps and branching in directions A and B. Even though the umbrella restraint does not impose any directionality, it is not possible for the substrate to migrate from one path to another due to the large energy barrier that the protein imposes on this migration at all but the very shortest restraint distances. Again, full equilibration of the solvated protein in conformational space was monitored for these steps.

The distribution of δ values for each window was determined by using 0.1-Å-wide bins. For each window the system was equilibrated and the potential of mean force (PMF) calculated. The PMF profile for acetic acid or acetate ion diffusion was calculated by connecting two consecutive windows at the point where the probability density, $p(\delta)$, was >5% for the two windows in the overlapping region. Starting with the second window, at 3.5-Å distance between Ser Oγ and carbonyl carbon, parallel simulations were carried out for acetic acid and acetate ion.

Full MD Simulations. The entire equilibrated protein including all solvate water was used. Acetic acid and acetate ion in different orientations were incorporated into the protein and minimized to eliminate bad contacts. This was followed by MD simulations at 300 K for 80−170 ps. Four different starting orientations, including the starting structure for umbrella sampling, were studied for acetic acid release. None of these led to migration via the alternate channel but through the main gorge. Acetate ion in some orientations engages in electrostatic interactions with residues in the oxyanion hole at close contact. Migration was thwarted when starting with these orientations. This is consistent with the ~10 kcal/mol barrier observed when umbrella sampling was used with these starting structures. However, three different orientations of acetate ion, including the one used in the first window for umbrella sampling, led to migration through the alternate channel and none through the main gorge. Migration was particularly fast (<50 ps) from the orientation obtained in the window at $\delta = 4.5$

(40) Durell, S. R.; Brooks, B. R.;; Ben-Naim, A. *J. Phys. Chem.* **1994**, *98*, 2198−2202.
(41) Steinbach, P. J.; Brooks, B. R. *J. Comput. Chem.* **1994**, 15, 667−683.
(42) Bernstein, F.; Koetzle, T. F.; Williams, G. J. B.; Meyer, E. F., Jr.; Brice, M. D.; Rodgers, J. R.; Kennard, O.; Schimanouchi, T.; Tasumi, M. J. *J. Mol. Biol. Chem.* **1977**, 112, 535.
(43) Brunger, A. T.; Karplus, M. *Proteins: Struct., Funct., Genet.* **1988,** *4*, 148−156.
(44) Bencsura, A.; Enyedy, I.; Viragh, C.; Akhmetshin, R.; Kovach, I. M. In *Enzymes of The Cholinesterase Family;* Quinn, D. M., Balasubramanian, A. S., Doctor, B. P., Taylor, P., Eds.; Plenum Press: New York, 1995; pp 155−162.
(45) Bencsura, A.; Enyedy, I.; Kovach, I. M. *Biochemistry* **1995,** *34*, 8989−8999.
(46) Bencsura, A.; Enyedy, I.; Kovach, I. M. *J. Am. Chem. Soc.* **1996**, *118*, 8531−8541.
(47) Reiher, W. E. Ph.D. dissertation, 1985.
(48) Loncharich, R. J.; Brooks, B. R. *J. Mol. Biol. Chem.* **1990,** *215*, 439−455.
(49) Steinbach, P. J.; Brooks, B. R. *Proc. Natl. Acad. Sci. U.S.A.* **1993,** *90*, 9135−9139.
(50) Brooks, C. L., III; Karplus, M. *J. Chem. Phys.* **1983,** *79*, 6312−6325.
(51) Brooks, C. L., III; Karplus, M.; Pettitt, B. M. In *Proteins: A Theoretical Perspective of Dynamics, Structure and Thermodynamics;* Prigogine, I., Rice, S. A., Eds.; Willey & Sons: NewYork, 1988; pp 38−44.
(52) McCammon, J. A.; Harvey, S. C. *Dynamics of Proteins and Nucleic Acids;* Cambridge University Press: Cambridge, 1989; pp 1−234.
(53) Nakagawa, S.; Yu, H.-A.; Karplus, M.; Umeyama, H. *Proteins: Struct., Funct., Genet.* **1993,** *16*, 172−194.

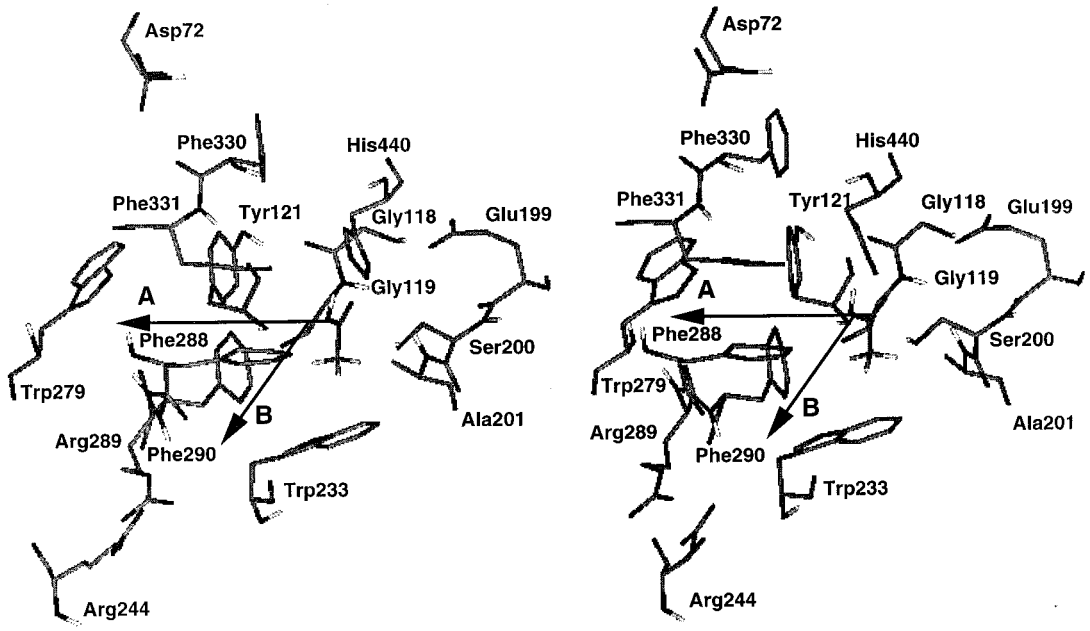

Figure 1. Starting orientation for acetic acid in the direction of (A) the entrance to the main gorge and (B) the alternate channel.

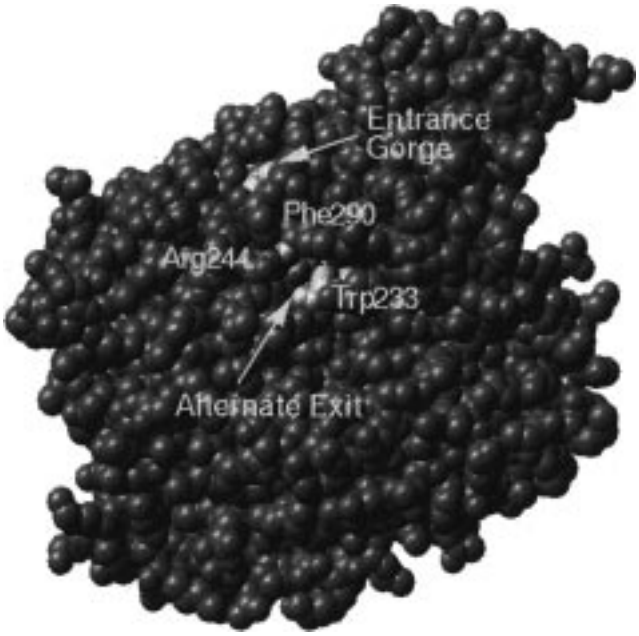

Figure 2. The *Tc* AChE monomer with the main gorge and the alternate exit for product release.

Å in the alternate channel. The migration of acetate ion through the main gorge could only be affected when acetate ion was placed at 4.5 Å from Ser200 Oγ and oriented with the carboxylate group in the direction of the entrance to the gorge.

Results

Two Reaction Pathways. Figure 2 illustrates the proposition for two possible exit routes for acetic acid or acetate ion. The obvious questions are the energy profile and dynamic characteristics of the migration of these products through the proposed entrance channel in the direction of the peripheral anionic binding site for substrates. Another route opens for the migration of products, particularly acetate ion. This route is located under the acyl binding site toward a groove region lined with positively charged Arg residues; the energetics of migration through this passageway is then the other issue.

Umbrella Sampling. The protocol that had been applied successfully to the escape of dioxygen from myoglobin[25,29,30] was adopted in our work for the calculation of the PMF. The PMF was calculated from the distribution, $\rho(\delta)$, of δ values:

$$W(\delta) = -k_B T \ln \rho(\delta) - U(\delta) + C_i$$

where C_i is a constant for a specific window. Each window "opened" at the end point of the previous simulation, the system was equilibrated in the new biasing potential for 10 ps and then was sampled for 70−90 ps, in 10-ps intervals, except for the last windows which were equilibrated for 40−50 ps. A new velocity started at every 10 ps to further probe if equilibration had been achieved. The overlapping windows provided a continuous function to determine the constants C_i.

Ionization of Acetic Acid in the Protein. A critical question in the evaluation of the exit of acetic acid from the protein is the point of ionization. If diffusion of acetic acid out of the protein is faster than ionization, the lower energy pathway for acetic acid migration will be preferred and ionization will have no effect on the course taken. The question is then if ionization of acetic acid can occur instantly at the active site. The early conformations of acetic acid at δ 3−4 Å were analyzed in search of potential proton acceptors. A strong possibility for proton loss is to the catalytic His440, which should be in the basic form after having completed the classic proton shuffling in the catalytic cycle (Scheme 1). The distances and angles for proton transfer to the lone pair of Nϵ on His440 are provided in Table 1. Clearly, the geometries at δ < 3.5 Å are ideal for proton transfer to His440, but the energy barrier depends on the relative p*K*s of acceptor and donor. Is such proton transfer thermodynamically favored? First, the electrostatic environment at the active site may be more polar than customarily believed. Strong arguments in favor of this contention can be found in Warshell's work.[26] Additionally, protonation of His440 has recently been considered to be promoted by surrounding carboxylates, Glu327 and Glu199.[19,20,54] Sheiner has delineated the angular aspects of proton transfer in protein interiors that can compensate for

(54) Radic, Z.; Kirchhoff, P. D.; Quinn, D. M.; McCammon, J. A.; Taylor, P. *J. Biol. Chem.* **1997,** *272*, 23265−23277.

Table 1. Distances (Å) and Angles (deg) between Potential H-Bond Acceptors and Donors Including Acetic Acid (AC) at the Active Site of *Tc* AChE at Different Values of δ (Å)

		δ			
donor	acceptor	2.98	3.18	3.62	3.83
His440 Nϵ	01 AC	2.82	2.90	3.21	3.86
His440 Nϵ	HO AC	1.83	1.90	3.21	3.86
His440 Nϵ	HO AC[a]	169	162	39	56
His440 Nϵ	Oγ Ser	4.26	3.90	3.25	2.89
His440 Nϵ	HO Ser	4.08	3.89	2.51	1.92
Tyr121 OH	02 AC	4.82	4.29	1.96	1.93

[a] Angle; all others distances.

the effects of a low dielectric.[55] These facts are in favor of proton transfer from acetic acid to His440 immediately after completion of the double displacement catalytic cycle. Should the proton transfer to His440 occur within picoseconds, acetate ion would be the product to migrate out of the protein. One might consider if the loss of the proton from His440 to another acceptor can also occur on a faster than the microsecond scale, the time scale for AChE catalysis, to restore His440 into the catalytically competent form. It seems likely, but a definite answer to this question cannot be offered at this time.

On the basis of the assumption that the p*K*s of acetic acid and His440 are matched at $\sim$<3.5 Å and proton-transfer catalyzed by His440 takes place rapidly, the PMF profile for migration for acetic acid and acetate ion were connected at $\sim$ 3.5 Å.

The First Three Windows. When restrained at close range from Ser200 Oγ ($\delta = 2.8-4.3$ Å), both acetic acid and acetate ion engage in a H-bond either in the oxyanion hole or with Tyr121 OH after 20−35 ps in the main gorge (Table 1). A H-bonding interaction with Tyr121 OH also occurs in the alternate channel under the same conditions. If the orientations leading to the interactions in the oxyanion hole had relevance to the migration of acetic acid/acetate ion, that would create a barrier up to 10 kcal/mol. If, however, acetic acid or acetate ion simply tumbles out from the starting orientation as derived from the quasitetrahedral transition state for the hydrolysis of the acetyl enzyme, then H-bonding to Tyr 121 OH occurs.

Migration Through the Main Gorge. The PMF profiles for acetic acid migration were calculated from its nascent state until the energies reached a plateau at 8 Å from Ser200 Oγ in the main gorge; shown in Figure 3A. There is a weak H-bond between acetic acid and the OH of Tyr121 in the main gorge. A barrier of <1.5 kcal/mol is observed at 6 Å from Ser200 Oγ. The PMF profile for the migration of acetate ion, shown in Figure 3A by dashed line, drops more rapidly than for acetic acid. The negative electrostatic gradient repels acetate ion more than acetic acid until the constriction formed by Tyr121, Phe290, Phe330, and Phe331 at $\delta = 10$ Å. The trend is nearly reversed at the constriction because of the repulsive effect of the peripheral anionic site, Asp72. There is also a small, $\sim$1.5 kcal/mol, barrier along this pathway for acetate ion at the choke point at $\delta = 10$ Å. At $\delta = 14$ Å, acetate ion reaches the solvent interface in the main gorge.

Not surprisingly, acetate ion interacts with protein residues and solvate water that stabilize it $\sim$100 kcal/mol more favorably than acetic acid in either passageway; this is shown for the main gorge in Figure 4. A prominent feature of the simulations was the "assistance" provided by Tyr121 to the departing acetic acid or acetate ion through the main gorge. Time series show that the H-bonding interaction is established between the HO of

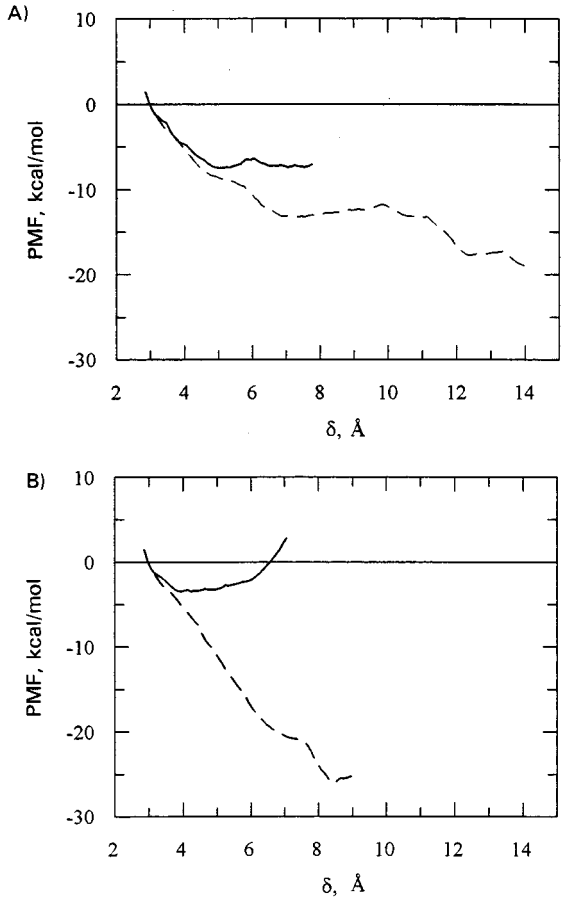

Figure 3. PMF profiles for acetic acid (solid line) and acetate ion (dashed line) through the (A) main gorge.(B) the alternate exit.

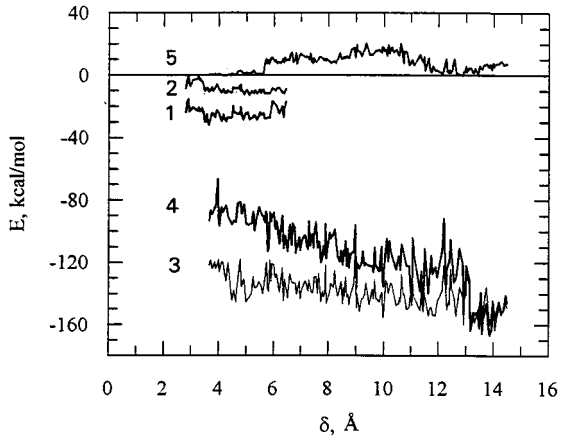

Figure 4. Potential interaction energies for acetic acid (1 and 2) and acetate ion (3, 4, and 5) with active-site residues and water in the main gorge during umbrella sampling; lines 1 and 3 indicate the total interaction energy; lines 2 and 4 indicate interaction energy with water; and line 5 indicates the interaction energy with Asp72.

Tyr121 and acetic acid after 35 ps simulation in the first window. The interaction is instantaneous with acetate ion in the second window. Figure 5 is a pictorial representation of the interaction of acetate ion with HO of Tyr121 after 40 ps simulation and at 4.5 Å from Ser200 Oγ in the main gorge. The interaction (potential) energies for acetic acid and acetate ion with Tyr121 are displayed in Figure 6. The interaction between Tyr121 OH and the acetyl fragment promotes departure until the fragment reaches the constriction formed by Tyr121, Phe290, Phe330, and Phe331. The RMSD for these residues is small, <2 Å,

(55) Scheiner, S. *Acc. Chem. Res.* **1994,** *27,* 402−408.

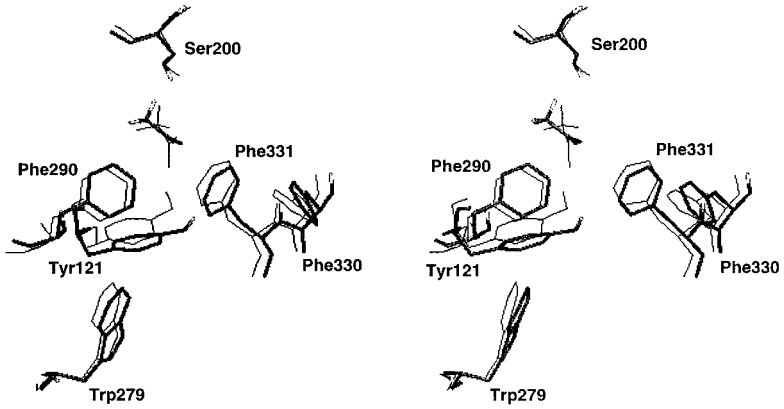

Figure 5. Pictorial representation of the interaction of acetate ion with Tyr121 OH after 40 ps simulation at $\delta = 4.5$ Å in the main gorge. Heavy lines indicate the starting structure, and thin lines indicate the last structure.

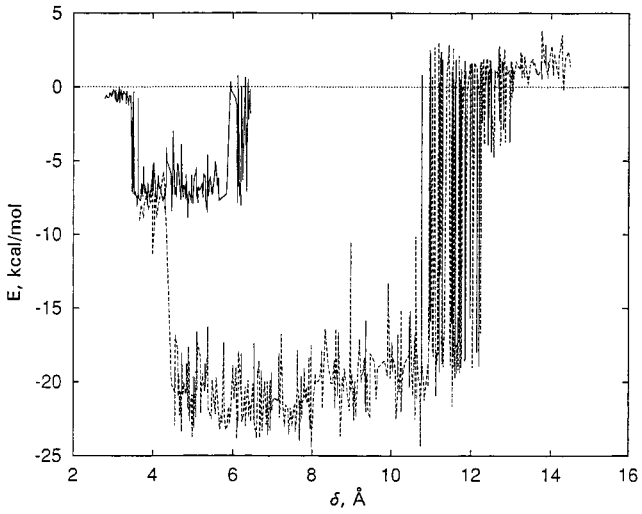

Figure 6. Interaction energies with Tyr 121 OH during umbrella sampling are indicated; solid line for acetic acid and dashed line for acetate ion in the main gorge.

while acetate ion diffuses out. The H-bond needs to be broken at the choke point. An MD simulation of the migration of unionized and ionized acetic acid shed further light to this problem (vide infra). A large breathing motion, RMSD up to 3 Å, was also observed for the most mobile, Gln74 − Phe78, segment of the Ω loop, which is consistent with a recent report of Wlodek et al.[20]

Migration through the Alternate Channel. The free energy of acetic acid passage in the direction of Arg244 was calculated until it encountered a barrier of 6 kcal/mol (Figure 3B). The barrier in the alternate exit channel is attributable to a H-bond of acetic acid to the carbonyl of Glyl19 or Phe292. Starting at 4 Å, the alternate channel provides a rapid fall of energy; $\Delta G \approx -16$ kcal/mol at 8 Å for the migration of acetate ion. A large motion of Phe290 with RMSD up to 4 Å is observable as acetate ion leaves the active site and leaves the protein. Trp279 near the peripheral anionic site becomes more mobile as acetate ion reaches the exterior of the groove. This motion appears to be associated with that of Phe290. At $\delta = 9$ Å, acetate ion reaches the solvent interface in the alternate channel.

A significant driving force for the diffusion of acetate ion through the alternate channel is an electrostatic attraction in the direction of two Arg residues, 244 and 289, near the groove region. This is lacking for acetic acid. The interaction energies between acetic acid and residues in the alternate channel hover around −20 kcal/mol, whereas for acetate ion they are around −100 kcal/mol. The RMSD is almost constant for Arg244 but not for Arg289 which fluctuates between 0.5 and 2.3 Å as acetate ion moves close to the residue. A large deviation of the Ω loop andTrp84 with it has also been noticed as acetate ion approached Arg244.

Table 2. Total, Main Chain (MC), and Side Chain (SC) RMSD Calculated for the Last 40 ps for Critical Residues Influencing Acetate Ion Migration through the Gorge and through the Alternate Exit

	gorge			alternate exit		
residue	total	MC	SC	total	MC	SC
Asp72	1.34	0.91	1.51	1.01	0.78	1.10
Trp279	0.78	0.56	0.83	1.99	1.31	2.13
Tyr121	0.56	0.33	0.62	0.70	0.59	0.73
Phe330	0.26	0.29	0.26	0.87	0.45	0.98
Phe331	0.93	0.27	1.07	0.58	0.45	0.62
Phe290	0.78	0.75	0.79	2.68	1.42	2.99
Phe288	0.27	0.16	0.30	0.37	0.29	0.39
Trp233	0.31	0.25	0.33	1.51	1.50	1.52
Arg244	0.89	0.74	0.93	0.91	1.12	0.84
Arg289	0.57	0.27	0.64	0.61	0.51	0.63

Full MD Simulations. Results of these simulations were ideal for the evaluation of trajectories for product clearance and for probing the results of the umbrella sampling method. The entire active-site region was monitored for correlated motions of active-site residues and openings for the release of ions. The RMSD for critical residues (vide supra) in each pathway is provided for the last 40 ps in Table 2. Figure 7 illustrates that the side-chain deviation of Arg244 is larger than the main-chain deviation, as might be expected, until acetate ion reaches a distance of ∼6 Å between the carbonyl carbon and Arg244 Nη; the trend then reverses. This reflects the effect of the approaching acetate ion on the positively charged guanidinium side chain of Arg244. The guanidinium side chain becomes increasingly engaged in an electrostatic-interaction with acetate ion which restricts its motion. Apparently, the Cα makes adjustments to the global breathing motion of the protein. Figure 8 summarizes the movement of acetic acid and acetate ion through the two pathways followed for upto 170 ps. Results of the full simulation are consistent with the results of the stochastic boundary method used with umbrella sampling. Shown in Figure 8A, acetic acid moves from 3.5 to 5.5 Å from the Ser200 Oγ in the first 80 ps in the main gorge. However, acetate ion is still at 8 Å, from a starting point of 4.5 Å, after 160 ps due to the electrostatic repulsion by Asp72 in the main gorge. Acetate ion reaches the solvent region 9 Å from the active site Ser200 Oγ through the alternate exit in <100 ps and leaves the protein completely at 170 ps.

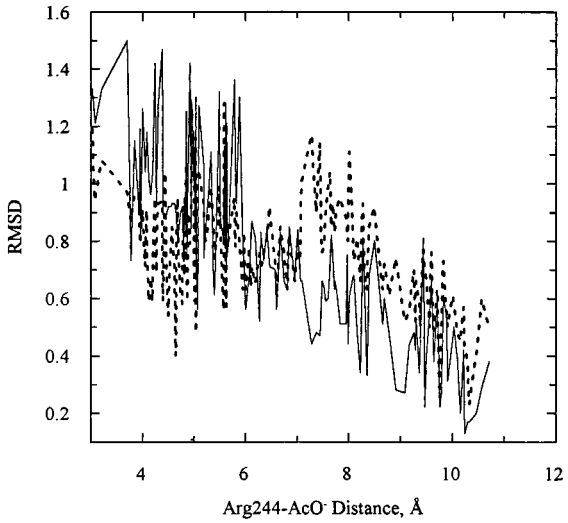

Figure 7. Comparison of main chain (solid line) and side chain (dashed line) RMSD values for Arg244 during acetate migration through the alternate channel.

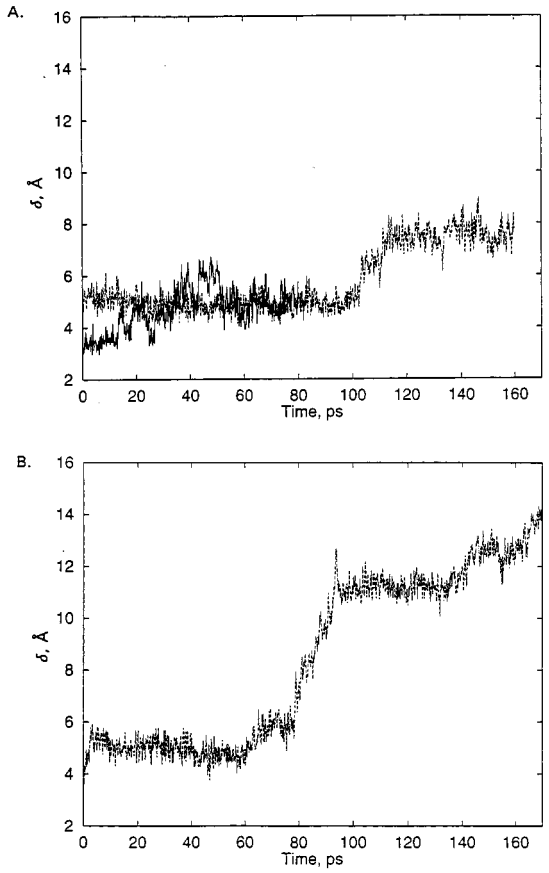

Figure 8. Full MD simulations (A) in the main gorge and (B) in the alternate channel for the migration of acetic acid (solid line) and acetate ion (dashed line).

Figure 9 shows patterns of migration of acetic acid through the main gorge. The barrier in the main gorge is due to the constriction created by the side chain of Tyr121, Phe290, Phe330, and Phe331. H-bonding to the side chain of Tyr121 is the determining factor in slowing product release through the constriction. The motion of the side chain of Tyr121 is correlated to the motion of the indole ring of Trp279. The cross-correlation coefficient for atomic fluctuation around the average for the motion of the indole ring of Trp279 and the phenyl ring of Tyr121 is 0.335 for the last 80 ps. The correlation diminishes toward the end of the simulation as the H-bond between Tyr121 and acetic acid is broken. The H-bond to the acetyl fragment can break when the acetyl fragment becomes solvated.

Acetate ion release through the alternate channel, illustrated in Figure 10, is facilitated by electrostatic interactions with Arg289 and Arg244, but slowed by small van der Waals interactions with the mobile side chains of Phe290 and Phe288. The interaction with Arg289 dominates for $9 < \delta < 12$ Å beyond that the interaction with Arg244 is stronger.

Discussion and Conclusions

Molecular dynamics calculations including the use of umbrella sampling located the lowest energy pathway for the migration of acetic acid or acetate ion out of *Tc* AChE from several orientations. The reaction coordinate for umbrella sampling is only a distance quantity without imposed directionality. There is no assumption that a given pathway is straight, but only that each pathway involves continual increases of the restrained distance. The directionality of a given path is imposed by the potential energy surface and the inability of the protein to completely rearrange on the time scale of the simulation.

The lowest energy pathway is for acetate ion migration through the alternate exit channel. The trajectories show very small if any free energy barrier to the migration of acetic acid or acetate ion. This result renders unlikely that viable pathways remained undetected. The most salient result of these calculations is that *if acetic acid can ionize in the first 20 ps and within 3.5 Å of the active site Ser Oγ, it probably just diffuses out of the enzyme in the direction of Arg289 and Arg244 into a well-solvated groove* (Figure 8). This route is 6 Å shorter than the one through the main gorge. A requirement for ionization of acetic acid is a dielectric environment quite similar to water. If however, acetic acid should remain un-ionized, it would probably migrate through the main gorge with some assistance from Tyr121. The small 1.5 kcal/mol barrier to migration through the main gorge may also be eliminated by motions correlated to catalysis of bond breaking and the release of the choline fragment perhaps through the "backdoor".[14]

Implications to the Mechanisms of Deacylation in Cholinesterases. A barrierless migration of larger acyl fragments from AChE should not be expected. The activation free energy for deacetylation at 25 °C and neutral pH is 11.8 kcal/mol,[56] which implies that product release can become rate limiting if a barrier of similar height is to be passed when a larger acyl fragment diffuses out of AChE.

The following experimental observations may be indicative of product release becoming partly rate limiting for large acyl fragments or if the passageway for acetic acid release is altered by mutations. Mutations in Mo AChE (number in parentheses is the equivalent in *Tc* AChE) in residues Phe295Tyr (288), Phe297Tyr (290), and Arg296Ser (289) decrease the value of k_{cat} 25-, 10-, and 2-fold, respectively.[57] Whereas Mo AChE has 200 times smaller k_{cat} value for the hydrolysis of butyrylthiocholine than for acetylthiocholine, its mutations Phe295Leu (288) and Phe297Ilu (290) result in significant enhancement, 54−70 times, in preference for butyrylthiocholine.[58] The absolute value of k_{cat} for acetylthiocholine falls by 4−6-fold

(56) Kovach, I. M. *J. Enzyme Inhib.* **1988,** *2,* 199−208.
(57) Radic, Z.; Pickering, N. A.; Vellom, D. C.; Camp, S.; Taylor, P. *Biochemistry* **1993**, *32,* 12074−12084.
(58) Vellom, D. C.; Radic, Z.; Li, Y.; Pickering, N. A.; Camp, S.; Taylor, P. *Biochemistry* **1993**, *32,* 12−17.

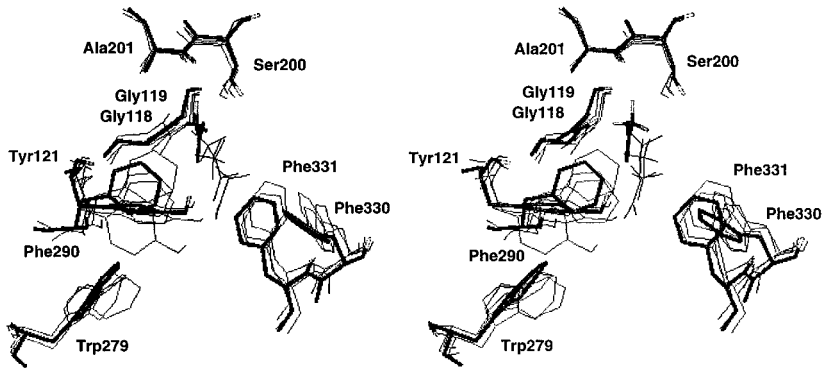

Figure 9. Patterns of migration of acetate ion through the main gorge during MD simulations: the starting structures are represented by the heavy lines, and the structures in thin lines illustrate successive orientations during simulation.

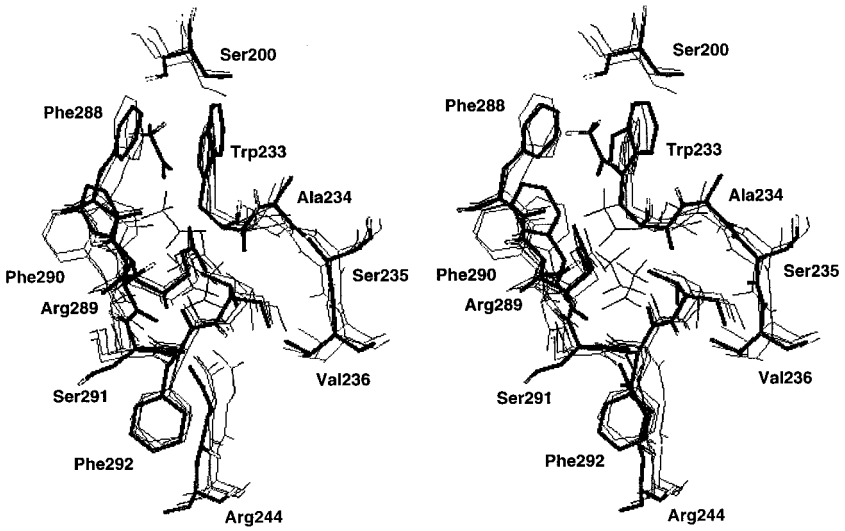

Figure 10. Patterns of migration of acetate ion through the alternate exit during MD simulations: the starting structures are represented by the heavy lines and the structures in thin lines illustrate successive orientations during simulation.

with the mutants, but rises for butyrylthiocholine ~12 times in each case. Similar mutations, Phe295Leu or Ala and Phe297Val or Ala cause an enhancement of 4−10-fold, respectively, in the value of k_{cat} for the hydrolysis of butyrylthiocholine catalyzed by human (Hu) AChE.[59]

Preliminary results of studies designed to probe the alternate channel indicate that the k_{cat} values for substrates hydrolyzed by butyrylcholinesterase decrease ~5−10-fold in Arg244Leu mutations of the enzyme.[60]

The two Phe residues in the acetyl binding site appear to wedge the methyl portion of the acetyl group[8] and, after C−O bond fission, yield easy passage of the product by their side-chain motions. Mutations in the acyl binding site of AChE result in adoption of the larger butyryl fragment and then may facilitate its release due to greater rotational freedom of the aliphatic side chain. At least two favorable effects of the mutations in the acyl binding site on hydrolysis of the butyryl fragment in deacylation can be envisioned: (1) Optimal binding can facilitate bond breaking between Ser200 Oγ and the carbonyl C. (2) Optimal interactions and side-chain motions may promote, or at least not inhibit, passage of products through the short route toward Arg289 and Arg244.

The attack of water on the acyl enzyme, which may require a small conformational change of the catalytic His440,can be coupled with product release.[56] The energy cost of a conformational change may be well invested if it implements a unidirectional flow from reactant to product, toward the increasing local negative electrostatic gradient for choline release and through a short alternate exit for acetate release.

In summary, a "conducted tour" across the protein might be enforced by the strong dipole of AChE. Specific orienting effects in the microenvironment of the active site further enforce a minimum energy reaction pathway for substrate(s) as well as covalently binding inhibitors. It is quite likely that two pathways are available for the acetyl fragment, main gorge exit (20 Å) and alternate exit (14 Å), but one becomes favored under some conditions and the other may be preferred under other conditions. Products of hydrolysis of unnatural substrates and inhibitors may also leave through one of the two passageways depending on their charge and size or the conformational change they produce.

Acknowledgment. This research was supported by the National Science Foundation through grants MCB9205927 and MCB940020P Pittsburgh Supercomputing Center and by Research Fellowship 1 F33 AG05742-01 from NIA/NIH for sabbatical research of I.M.K.

JA973131H

(59) Ordentlich, A.; Barak, D.; Kronman, C.; Flashner, Y.; Leitner, M.; Segal, Y.; Ariel, N.; Cohen, S.; Velan, B.; Shafferman, A. *J. Biol. Chem.* **1993**, *268*, 17083−17095.

(60) Viragh, C.; Kovach, I. M.; Lockridge, O. Unpublished result.